Chapter 2

2.1 Asymmetrical liquid crystals cells

The invariability of NLC for director inversion leds to a no polarity sensitive electrooptical response of a NLC cells subjected to an external electric field. For instance, when a square wave is applied on the electrodes of a NLC cell with the molecular director previously oriented parallelly to the confining plate, a pulsed symmetric electrooptical response with halved period respect to the applied voltage is observed (fig. 1).

Few years ago a new method has been developed to achieve the polarity sensitive electro-optical response in nematic [1,2] and ferroelectric [3] liquid crystal cells. It consists of the insertion of mixed conductor film as electrode, deposited using different techniques such as evaporation, sputtering, sol-gel coating, etc. The first material checked for such devices has been the tungsten trioxide (WO_3) [1,2]. Its electrochemical properties are well known and it is widely used in electrochromic devices. The basis of polarity-sensitive electro-optic response is related to the different results of the ionic diffusion process, which

takes place in the WO_3 electrode during the anodic and cathodic polarization (for a better understanding of the matter, it's convenient, for the following discussion, to define the electric polarization with respect to the electrode made by the mixed conductor film). For instance, in case of anodic polarization, under the action of a low-frequency external electric field, the free charge carrier (H^+), always present in these films [4], migrates towards the oxide-liquid crystals interface, giving rise to a reverse internal electric field, which counteract the reorientation of NLC molecules. The same model has been qualitatively applied to more complex systems, based on mixed films of different oxides such as V2O5/TiO2, with variable atomic ratios, obtained via sol-gel route. NLC cells assembled with a thin titania-vanadia film (prepared at pH=1) on one electrode show a polarity- sensitive electro-optic response similar to the one reported for WO_3 cells, with the reorientation of NLC molecules inhibited by an internal electric field during the anodic polarization [5].

For these aims, many efforts have been made in recent years in order to find materials with electro-optic response qualitatively opposite to the WO_3 one. Mixtures of V_2O_5 and Bi_2O_3 have been investigated and some results were reported in literature very recently [6]. Unfortunately the optical contrasts

provided by such devices were low and no model was reported to explain the new effect.
However, many experimental evidences collected in the course of such investigations suggest the importance of chemical details during the sol gel route to determine the structural and conductivity properties of the films: in particular the annealing temperature at which the mixed oxide has been treated and, in the case of V2O5/TiO2, the pH values in the hydrolysis. In the present section, we report, as previous works collection, the main lasts results till now obtained besides to a brief description of the sol-gel thecniques used to synthetize the mixed oxide.

2.2 Tungsten trioxide

the tungsten trioxide has been among the firsts materials used to realize electrocromics devices because its good characteristics of both electronic and ionic conductor. This material show a quite complex polymorphism dependent by many factors as the distribution of the grain dimension, the thermal and mecanic hystory and so on. Another important characteristics of this films is the high presence of water, in fact the open and disordered structure

favourise the intercalation process of water molecules during the deposition process of the film.
The WO_3 tin film has been deposited by r.f. sputtering in A_r and O_2 atmosphere, the Oxigen/Argon ratiohas been mantained at 10% during the deposition. The samples has been subsequently annealed at 260°C. An other iteresting morphological characteristic of WO_3 is the columnar structure on little scale. Such structure is well visible in the AFM image showed in fig.2.2.1. In fig. 2.2.2 we have the electrooptical response of a NLC cell containing a WO_3 electrode annealed at 260°C compared with an electrooptical response of a standard NLC cell. The amplitude of applied sqare wave is 8V pic to pic and the frequency is 0.2Hz.

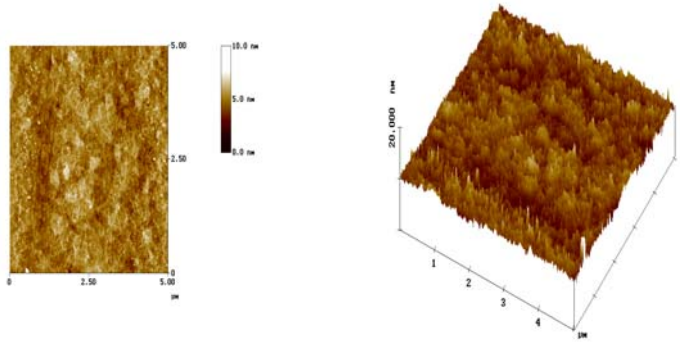

Fig.2.2.1) AFM image of WO_3 thin film.

(a)

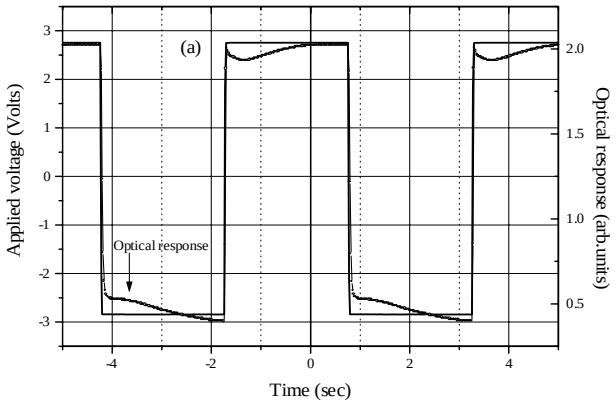

(b)

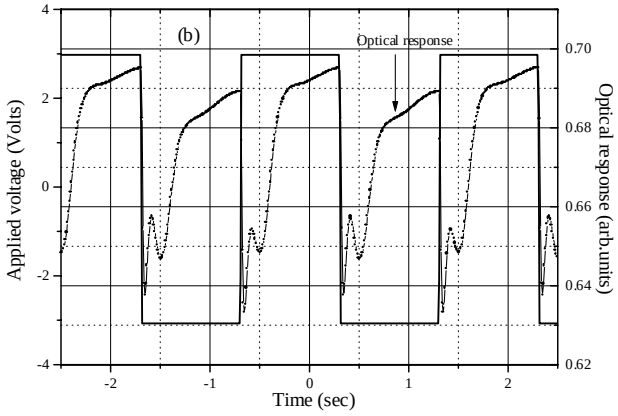

Fig. 2.2.2) Electrooptical response of a NLC cell containing WO_3 annealed at 260°C (a) and electrooptical response of a standard NLC cell

2.3 Sol-gel technique

The sol-gel process is a techniques wedly used to obtain various materials especially in form of dusts for ceramics and thin film. Among the advantage of this techniques its must to underline the semplicity in obtaining thin film on almost all kind of substrate, the low temperatures requiested during the preparation of the film, the fairly good cost and the possibility to have a good stechiometric control during the realisation of complex systems with an high degree of purity or, eventually, doped.
The sol-gel technique is founded on an opportune molecular solution which, by chemical reaction, transform itself to a colloidal solution (sol) and finally, after further chemical reaction, in a solid gel.
As precursor for the process are often used metallic alkoxide, the formula of such alkoxide is of the kind $M(OR)_n$ where M is the metal and R is the alchilic group. It is also possible to realize multicomponent systems using different alkoxide; one for every metal.
The sol is obtained dissolving opportune quantity of the various precursor in an organic solvent, usually alkool, afterwards, by hidrolisys and policondensation reactions, the gelification happen. The next step is that to eliminate the residual water and solvent by a

process of thermal drying. The evaporation of organic component lead to the formation of vacuum into the the film and then to the break down of the gel structure. The gel phase is cobstituted, usually, by an ordered structure only on first nearby scale. With the energy provided by the thermal treatment the atoms rearrange itself forming protocrystals of few nanometrs. Increasing the temperature is possible to obtain a further rearrange that lead to the protocrystals aggregation and then to the formation of crystalline clasters as son as bigger. The possibility to obtain crystalline clasters of nanometric dimension represent one of main interest of the sol-gel thecnique.

2.4 Titania/Vanadia thin film: sol-gel synthesis

V_2O_5/TiO_2 sols were prepared using the alkoxide route: titanium tetrabutoxide, $Ti(OBu)_4$, and vanadium oxo-triisopropoxide, $VO(OPr^i)_3$, were mixed with atomic ratio Ti/V 1/1. Such mixtures were allowed to react with acetic acid in a 1/1 molar amount for the chelation step; after the weak exothermic reaction took place, 2-propanol was added as a solvent, up to a 20/1 ratio to the metal

alkoxides amount. Hydrolysis reaction was carried out after 2 hours by adding an HCl aqueous solution, with a molar ratio 1/1 with respect to the total alkoxides amount.

Different pH values of the hydrolyzing solution were tested for various samples. In the present work samples made from the mother solution at pH=0 and pH=1 are analyzed and compared.

After a couple of hours, monolayered films were deposited on ITO (indium tin oxide)-glass (sheet resistivity ρ_s = 20 Ω/□, Unaxis GmbH) substrates by means of a dip-coating apparatus. The complete elimination from the films of the organic solvent was obtained via a drying procedure, occurring at temperatures not exceeding 120 °C. The films undergoing all these steps are defined “as grown samples”. Some of the films underwent a further annealing at 400 °C and at 500°C.

2.5 Raman measurements on Titania-Vanadia

It's well known that changes of chemical parameters during the sol-gel route affect the rate of crystallization of the materials generally amorphous after deposition at room temperature and desiccation. The degree of crystallization can change the ratio between ionic and electronic conductivity in the oxides generally used as electrodes [7]. For this reason the structural evolution of mixed titania-vanadia films grown at two different pH (0 and 1) has been comparatively investigated by using the micro-Raman spectroscopy.

The Raman spectra of TiO_2-V_2O_5 films were collected in several regions both for the series grown after pH=1 hydrolysis and for the series derived from a pH=0 process, starting with the as deposited films and monitoring the eventual spectral changes on the film after the annealing at 400° C and at 500°C.

In Figure 2.5.1 are shown some characteristic Raman spectra, from 200 to 1200 cm^{-1}, of the as-deposited sample made at pH=1 and at pH=0.

In most of the cases the specific Raman signal due to the films is quite weak, so that the substrate

contribution is largely dominant belonging to the different series. However, in the pH=1 samples, spots with strong signal at high frequency (800-1000 cm^{-1}) are quite common [8,9].
In both the kinds of samples the very broad bands typical of amorphous structure are observed. The main difference between pH=1 and pH=0 samples is the stronger signal of a broad band at about 920 cm^{-1} for the former ones. It has been assigned to vibrations of polyvanadates chains belonging to thin vanadium oxide layers in supported catalysts [10,11], but it also appears in the spectra of disordered vanadium pentoxide films grown in oxygen deficient environment or after intercalation processes [12]. The main spectral features of the latter samples, on the contrary, resemble the pattern of disordered titanium dioxide [13,14].
The annealing at 400 °C induces quite different transformations for the two classes of films with different chemical history, as it can be easily observed from the spectra of Figure 2.5.2
In fact, it’s quite evident that a well developed crystallization process for the pH=0 samples occurs. The sharp Raman peaks growing above the substrate contribution can be certainly assigned to well crystallized phases of vanadium oxide. However, the vibrational frequencies, hence the coordination, symmetry and bond lengths [15], seem to be slightly

different from those of the polycrystalline vanadium pentoxide [16-17]; it rather resembles the spectrum of the deformed structures derived from it, via lithiation processes [18,19].
On the contrary the other films show a clear spectroscopic evidence of a still amorphous or nanocrystalline structure. However, the strong high frequency component associated to polyvanadate chains seems generally decreased after the 400 °C annealing.
The thermal treatment up to 500 °C induces further modifications for both the classes of titania-vanadia films: in Figure 2.5.3 the representative spectra are shown. The Raman peaks due to crystalline V_2O_5 phases now are observed for both the kind of films, but in the pH=0 samples the well developed crystallization of TiO_2 into the anatase phase also appears as indicated by the occurrence of two sharp Raman peaks at 513 and 640 cm^{-1} [20]. No clear spectroscopic evidences for the crystallization of TiO_2 are found, instead, for the pH=1 samples. The low-medium range frequency spectrum is consistent with the occurrence of a residual mixed amorphous structure, where the growth of nanocrystalline phases of TiO_2 is also possible.

In conclusion, after the highest temperature annealing, the pH=0 samples structure consists of crystalline

phases of TiO_2 anatase and modified V_2O_5, well mixed on the scale of micron. In such system the ionic conductivity is expected to decrease, while the electronic conductivity is enhanced by the extended crystal size, as confirmed by the impedance measurements. Such process does not occur in the same extent in the pH=1 samples, so that, the ratio between ionic and electronic conductivity can results quite different. For these reasons the prevalent mobile charges can be different for the oxide films made at different pH and undergoing a different structural evolution after thermal treatment.

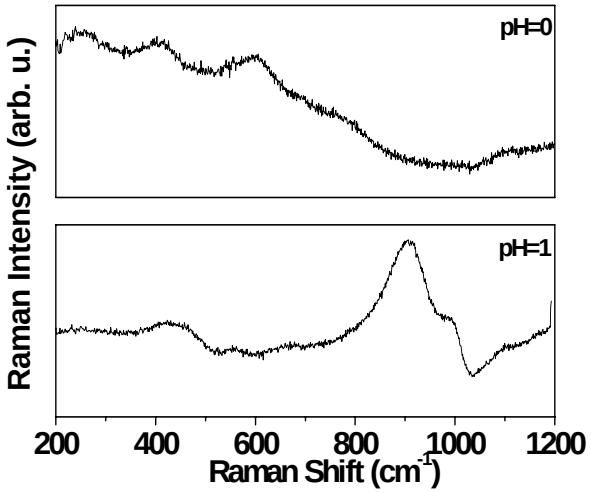

Fig. 2.5.1) Raman spectra of the as deposited samples, made at different pH.

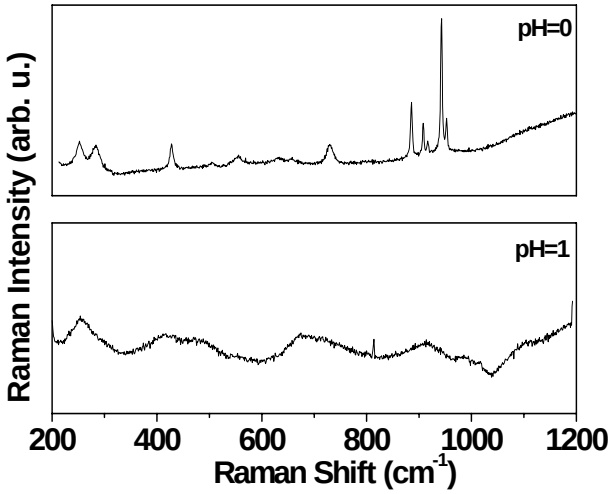

Fig. 2.5.2) Raman spectra of the samples annealed at 400°C.

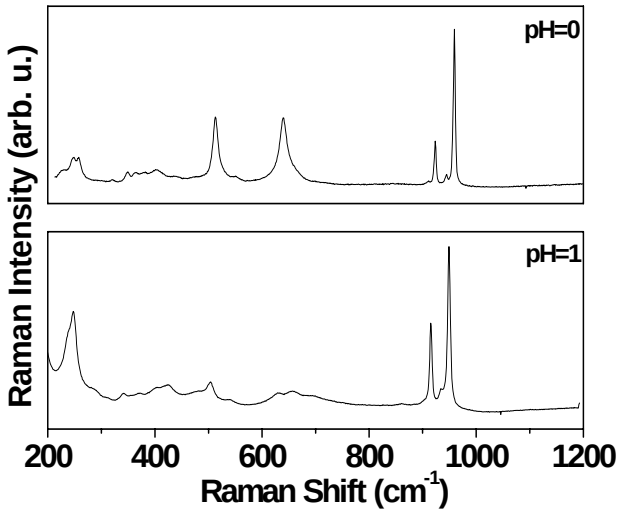

Fig. 2.5.3) Raman spectra of the samples annealed at 500°C

2.6 Electrical properties of Titania-Vanadia

The electrical properties of oxide titania-vanadia films have been investigated to determine its electrochemical properties. The conductivity of these films plays an important role in the electro-optic

behavior of the liquid crystals asymmetric cells. Measurements of the electric impedance have been performed both on as-deposited films and after each annealing step at 300°C, 400°C and 500°C. The electric properties of the film has been investigated using an impedence analyser Eg&G 273A. A complete description of the electric schema used to perform this measurement is reported on the next section addicted to the experimentals setups. The most remarkable finding for the mixed titania-vanadia films, grown at pH=0, is the dramatic decrease of the total impedance of the films as temperature increases (see Figure 2.6.1).

The measurement on the as-deposited films reveals very high impedance, of the order of $10^7\Omega$ at 1Hz, which monotonically decreases to $10^4\Omega$ at 10^4 Hz. The impedance of the film is reduced of three orders of magnitude after the first annealing at 300°C, while the shape of the curve is almost flat up to 10^4 Hz.
More detailed information can be obtained by separating the real and the imaginary part of the impedance of the film. We noticed a strong change in the frequency dependence of imaginary part, from a decreasing trend in the “as deposited” films to a very low value, with some increase toward the highest frequencies, for the annealed samples. The decrease of seven orders of magnitude is due to a strong reduction

of the out of phase component of the current flow through the oxide film. The real part also changes its behavior, from a monotonic decrease in frequency to a plateau for all the explored frequency range. The cut-off frequency probably occurs for higher frequency, above our measuring range, as suggested by the behavior of the imaginary part. This is the typical behavior of a pure electronic conductor. This transformation can be explained by a decrease, inside the film, of water molecules concentration and related ions, due to crystallization of the oxide, which is complete at 500 °C. In fact, both the electrical measurement and the changes of Raman spectra describe the same evolution of the material: i.e. the growth of microcrystalline phases out of an amorphous matrix, associated to a strong decrease of ionic conductivity and the establishment of a good electronic conductivity. In fact these oxide films, obtained by pH=0, have an ohmic resistance reduced of three orders of magnitude, while the capacitive reactance actually vanished (see Figures 2.6.2 and 2.6.3).

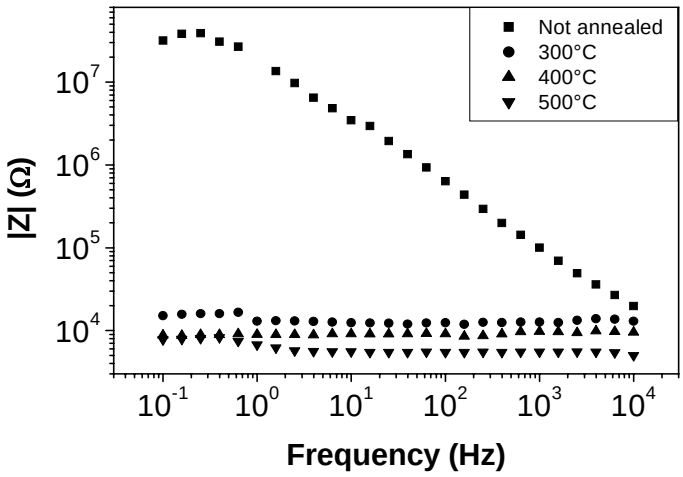

Fig. 2.6.1) Titania-vanadia film: impedance of not annealed film, compared with ones after each annealing step

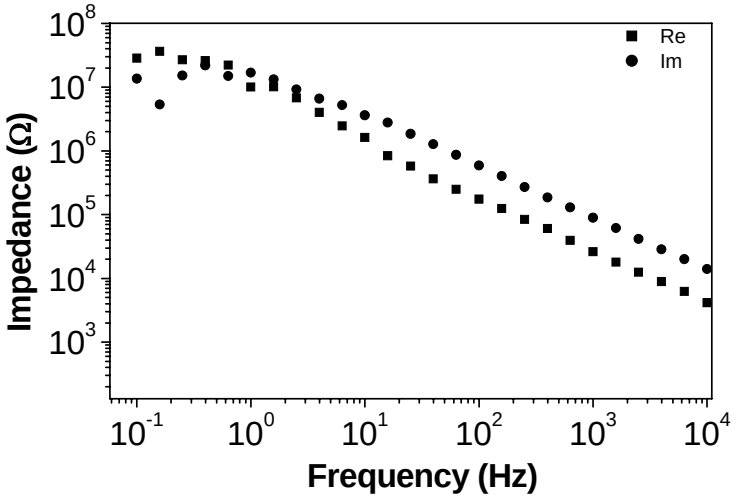

Fig. 2.6.2) Real and imaginary part of the impedance of as deposited " titania-vanadia film

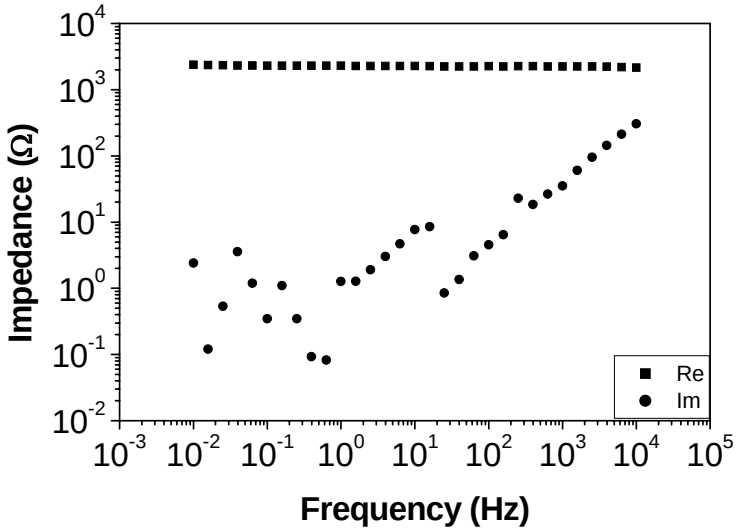

Fig. 2.6.3) Real and imaginary part of the impedance of annealed titania-vanadia film at 500°C

2.7 Electrooptic characterisation of LC cells containing Titania-Vanadia.

Asymmetric NLC cells have been prepared with both annealed and not annealed films.

NLC cells made asymmetric by inserting a titania-vanadia layer onto one of the electrodes show an electro-optic response dependent on the annealing treatments. The observed differences can be reasonably attributed to the changes in the film structure and conductivities, due to the annealing, as discussed above, and they are strongly dependent on the interaction with liquid crystals at the oxide-liquid crystals interface.

The time dependence of the optical transmission between crossed polarizers, can give an immediate qualitative check about the symmetric or asymmetric behavior of the NLC cell when a square wave electric field is applied. In absence of applied electric field, the NLC molecules were planarly aligned, i.e. aligned with the molecular director parallel to the boundary surfaces. The samples orientation was adjusted on microscope table so that a maximum of transmitted light was achieved.

Usually NLC cells with no special films inserted onto the electrodes exhibit a symmetric, impulsive-like, pattern of transmitted light signal through the cell. That behavior is basically similar to the one shown by NLC cell containing a not annealed titania-vanadia film (Figure 2.7.1). The small asymmetry present in the optical response is due to transient phenomena in the liquid crystals reorientation, but after 0.2-0.3 s the

transmitted light is almost the same for anodic and cathodic polarization.

The optical response of the cell changes after each annealing process of the titania-vanadia film inserted into the cell (films grown at pH=0). The best rectified squared electro-optic response was obtained for the inserted films annealed at 500°C (Figure 2.7.2); the optical transmission does not change for the cathodic polarization. It is worth to remark a difference in the sign of such rectification effect, with respect to the NLC cells containing titania-vanadia film prepared at pH=1, previously investigated [21]. In fact in the latter case the reorientation of NLC molecules was inhibited by an internal electric field during the anodic polarization (figure 2.7.3). The transient times are much shorter than for not-annealed films, and different for anodic and cathodic polarizations.

As for the asymmetric NLC cells previously studied [1-6], the rectification of electrooptic response has to be related to some internal electric counter field rising up inside the liquid crystals slab.

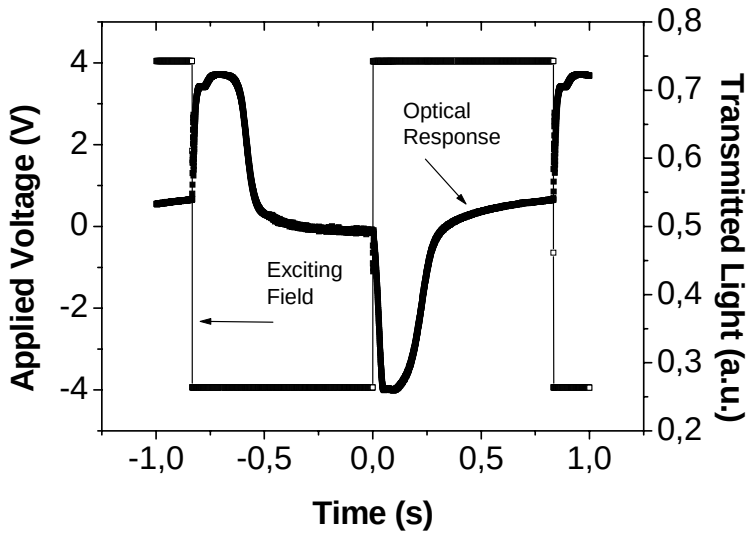

Fig. 2.7.1) Transmitted light through a nematic liquid crystal cell between two crossed polarizers, having one electrode coated with a sol- gel deposited not annealed titania-vanadia film (grown at pH=0). The value of voltage amplitude was 4 V. The behavior is basically similar to the one of usually NLC cells with no special films inserted onto the electrodes.

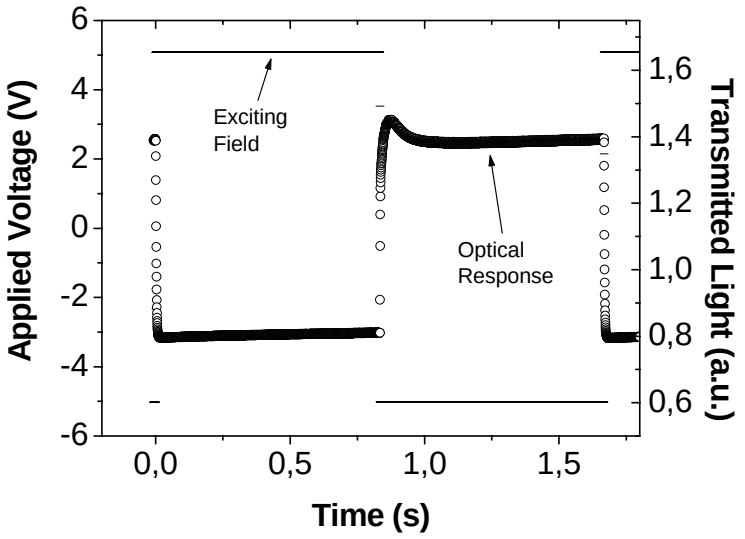

Fig. 2.7.2) Transmitted light through a nematic liquid crystal cell between two crossed polarizers, having one electrode coated with a sol- gel deposited film with Ti:V ratio of 1:1 grown at pH=0 and having undergone an annealing process at 500°C after Sol-Gel deposition. The value of voltage amplitude was 4.5 V

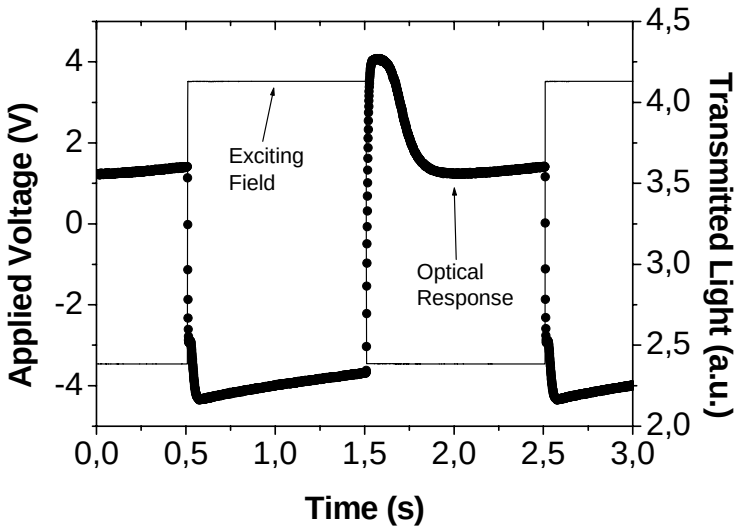

Fig. 2.7.3) The same of Figure 9a but using monochromatic light (He-Ne laser, 632).

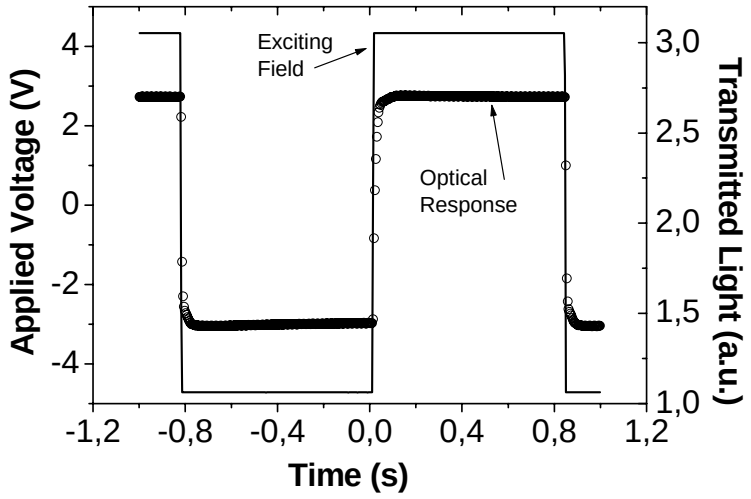

Fig. 2.7.4) The same for a nematic liquid crystal cell between two crossed polarizers, having one electrode coated with a sol-gel deposited film with Ti:V ratio of 1:1 grown at pH=1 and having undergone an annealing process at 400°C after Sol-Gel deposition.

2.8 Bismuto-Vanadia thin film: sol-gel synthesys.

Vanadium oxo iso-propoxide, $VO(OC_3H_7)_3$ was left to react with acetic acid in equimolar amount in a vessel under stirring and in nitrogen atmosphere. Then, 2-propanol was added as a solvent; to the obtained pale green solution, $BiCl_3$ dissolved in ethanol (95 %) was added, giving rise to a deep orange coloration; the atomic ratio Bi/V was kept to a 1/10 ratio. After a couple of hours, water was added in an alkoxide/water = 1/1 molar ratio; pH = 1 were used in this step. Films were deposited after one more hour on glass coated with Indium Tin Oxide (ITO), having an electric resistivity of 20 Ω/ , and on silica glass (optical grade), in both the cases with a withdrawal rate of 6 cm/min. Samples were dried at room temperature or at 120 °C; further heating to 400 °C for 1 hour, heating rate of 2 °C/min, was performed on selected samples.
During the hydrolysis step pH= 1 was used. Several characterizations have been performed on such resulting gels and on the deposited films.

2.9 Raman measurement on Bismuth-Vanadia

Optical microscopic investigation and micro-Raman analysis were performed on the deposited films, as grown and annealed. The signal on as-deposited film is very weak, except in some spot where thicker aggregates are found on the powders and.
In Fig.3 typical examples of micro Raman spectra are shown. Most of the film, in the homogeneous regions, show spectra as in Fig.2.9.1a, basically corresponding to ITO coated glass substrate. As found previously in titania –vanadia mixed films , that is an evidences of an amorphous structure, associate to a homogeneous deposition of the films generated by the sol-gel route with pH=1. In fact very thin films, lets say below 200 nm do not give appreciable Raman signal before the annealing. This is not due to experimental limits, because the same films show an appreciable signal when a complete crystallization is induced by high temperature heat treatments. In fig 2.9.1b and 2.9.1c the spectra near a thicker aggregate and just on it are shown. The relevant peak falls at about 810 cm^{-1}, indicating a structure of the bonds quite alike to that found in $BiVO_4$ films[18-20] . For other film samples the weak Raman signal generated by the thin homogeneous oxide layer was covered by a strong luminescence.

The 400 °C annealing induces an increase of the crystallinity of the films. In Fig. 2.9.2 some characteristic Raman spectra of an annealed film are shown. Spots on the aggregates or from the regions nearby give spectra as 2.9.2c and 2.9.2b, respectively, but even in the homogeneous region, far from the aggregate, a weak signal from a crystal phase like $BiVO_4$ can be detected, as in spectrum 4a.

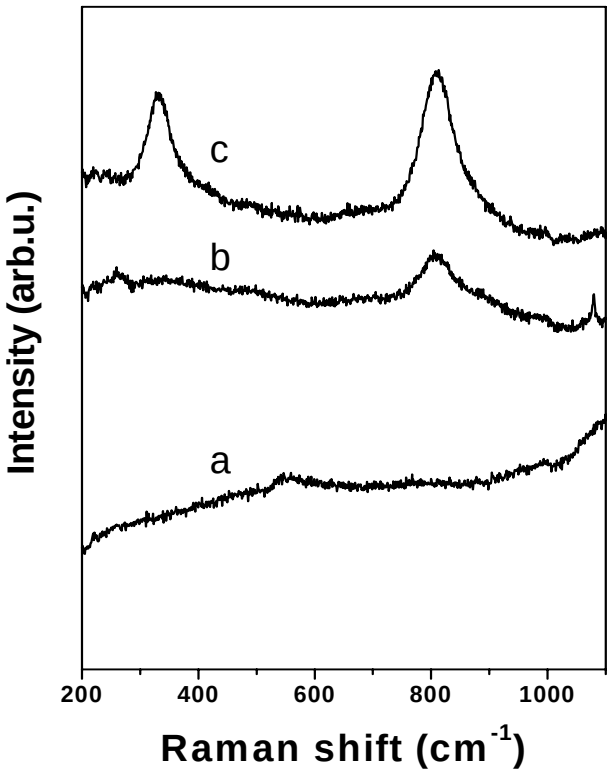

Fig. 2.9.1) Spectra from different spots of a micro-Raman mapping on a Bi/V =1/10 film, "as deposited". a) Spectrum from homogeneous thin film region. b) Collected in proximity of a thick aggregate. c) Collected at the center of the aggregate

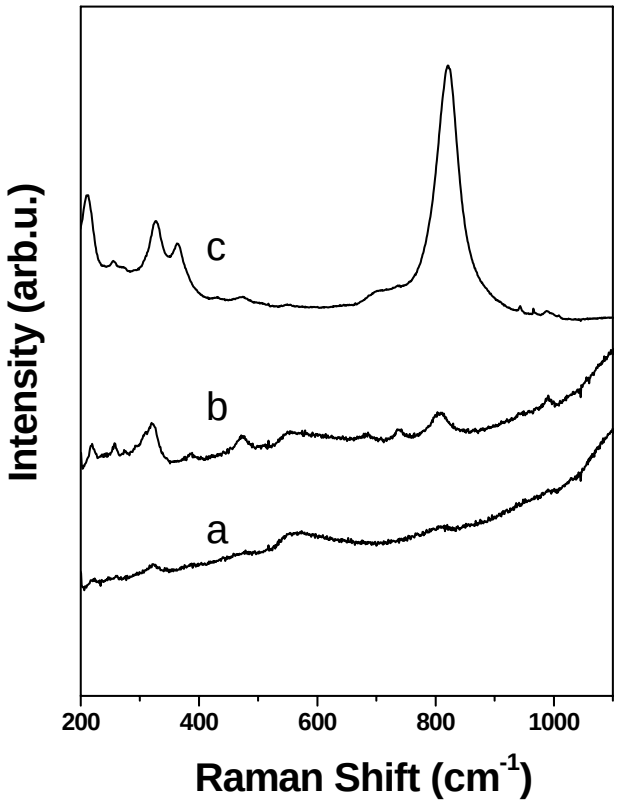

Fig.2.9.2) Spectra from different spots of a micro-Raman mapping on a Bi/V =1/10 film, after 1 h annealing at 400 °C a) Spectrum from homogeneous thin region, far enough from any aggregate. b) Collected in proximity of a thick aggregate. c) Collected at the center of the aggregate

2.10 Electrooptical characterization of LC cells containing Bismuth-Vanadia

The NLC cell containing “as deposited” Bi/V 1/10 film, exhibits an electro-optical behavior not very different from the symmetric cells above cited. The transmitted light change is impulsive-like, with a weak asymmetric response between anodic and cathodic polarization of the cell (see fig. 2.10.1). On the contrary, the NLC cell containing “400°C annealed” films with the same atomic ratio Bi/V shows a nice rectified square wave asymmetric response (see fig. 2.10.2) Besides the specific examples of Fig.6, the electrooptical response of NLC cell containing mixed Bi/V films has a complex dependence on the frequency of the square wave and on the values of applied voltage. In any case the annealed films have a more interesting response, with regard to the wanted rectifying effect

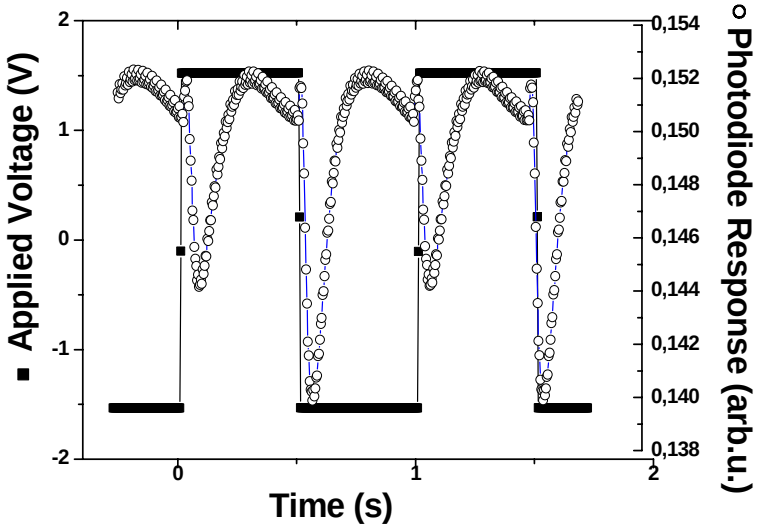

Fig. 2.10.1) Transmitted light through a nematic liquid crystal cell between two crossed polarizers (open circles), having one electrode dip-coated by a sol-gel film with Bi/V ratio of 1/10 , "as deposited". A square wave of 1.5 V amplitude, 1 Hz frequency, was applied (solid squares).

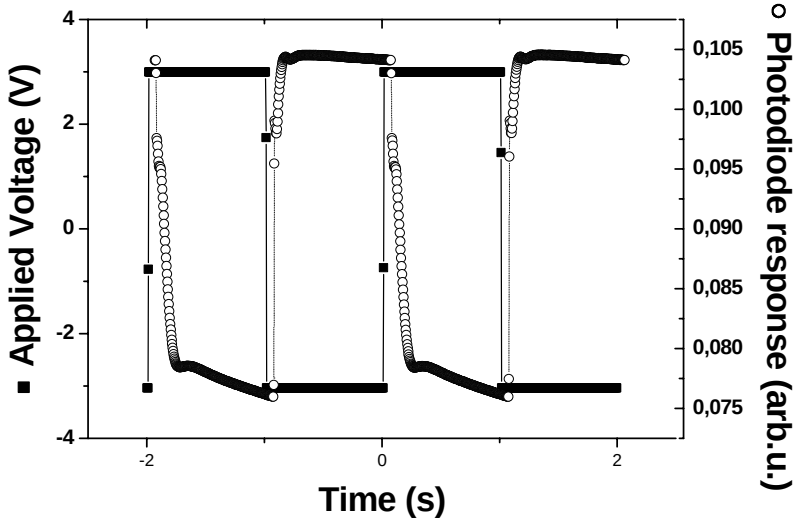

Fig. 2.10.2) Transmitted light through a nematic liquid crystal cell between two crossed polarizers (open circles), having one electrode coated with a sol-gel deposited film with Bi/V ratio of 1/10 , annealed at 400 °C . A 0.5 Hz square wave of 2.5 V amplitude was applied (solid squares).

2.11 Qualitatives interpretations

The most remarkable observation of all of this work is the correlation between the crystal order properties of the oxide films and the rectification effect in a nematic liquid crystal device. In fact The best performances in this regard has been obtained for films deposited by sol-gel methods and thermally treated at high temperatures. Moreover the electrooptical response obtained in the case of Bi/V and Ti/V (grown at pH=0) results to bee inverted respect to the electrooptical response previously obtained with the WO_3. This opposite effect could be explained, in principle, using the same model created for WO_3 and applied also to previously investigated Ti/V and Bi/V films: it should be enough to invert the sign of ions moving into the oxide and responsible of the counterfield created inside the cell.
Unfortunately there is no experimental evidence of significant current of negative ions inside these films, nor conduction of negative ions has been reported in literature about these materials. The present experimental studies suggest, on the contrary, an increasing role of conduction electrons for the

annealed films. On such basis, a phenomenological model of the effect can be proposed, taking into account the effects of thermal annealing upon ionic and electronic conductivity of the oxide. In the model created for the WO_3 films the ions H^+ play the main role in the creation of the a counterfield due to their abundance and to the columnar morphology of such oxide, that favorites ionic intercalation and deintercalation. In the case BI/V and Ti/V films, the annealing process eliminates completely water and the associated H^+ ions from the film, and no appreciable re-intercalation of water can occur after the crystallization process. The measurements of AC conductivity performed on the annealed films unambiguously showed that the conduction is almost electronic, and no frequency dependence is observed in the wide range investigated.

Let us consider the ITO electrode with oxide deposited on it. The electrons coming from ITO during the cathodic polarization can go through the oxide and accumulate at the oxide-liquid crystals interface because of the chemical potential barrier [1].

Now, we have to take into account the role played by the liquid crystal. If the liquid crystal were a perfect dielectric, when applying an electric voltage across the cell, the potential would vary linearly with distance and the electric field would be constant. On the contrary, if the liquid crystal contains a certain

amount of free ions, there will be a build-up of positive charge to the cathodic side of the cell and a similar build-up of negative charge on the other side. The electric potential will no longer have a linear dependence and the electric field will not be constant. It will present a lower value in the bulk of the liquid crystal layer and higher values close to the surfaces [4]. The negative charges are attracted on the other side on the liquid crystals by the ITO electrode charged positively. The larger are the boundary charges the higher are the values of the field near the surface and the lower is the field in the bulk of liquid crystals layer. These two boundary charges on the liquid crystals tend to screen the charges on mixed oxide - liquid crystal or ITO - liquid crystal interfaces. The consequence of this displacement of charge is a reverse internal electric field, which counteracts unipolarly the external perturbation; in such a way that a greater modulus of the external applied field is needed to reach the threshold for the reorientation of NLC molecules.

On the contrary for the anodic charge the same applied voltage is sufficient to trigger the optical switching, and that implies the absence or a strongly reduced density of any double layer creating an inner counterfield.

References.

[1] G. Strangi, D.E. Lucchetta, E. Cazzanelli,N. Scaramuzza C. Versace and R. Bartolino**;** Applied Physics Letters, **74 (4),** 534 (1999).

[2] E. Cazzanelli, N. Scaramuzza, G. Strangi, C. Versace, A. Pennisi and F. Simone; Electrochimica Acta, **44(18),** 3101 (1999).

[3] G. Strangi, C. Versace, N. Scaramuzza and V. Bruno; J. of Applied Physics, **92 (7),** 3630 (2002).

[4] G. Strangi, E. Cazzanelli, N. Scaramuzza, C. Versace and R. Bartolino**;** Physical Review, **E 62(2),** 2263 (2000).

[5] V. Bruno, E. Cazzanelli, N. Scaramuzza, G. Strangi, R. Ceccato and G. Carturan; J. of Applied Physics, **92 (9),** 5340 (2002).

[6] E. Cazzanelli, S. Marino, V. Bruno, M. Castriota, N. Scaramuzza, G. Strangi, C. Versace, R. Ceccato and G. Carturan; Solid State Ionics, **165,** 201 (2003).

[7] A. Antonaia, T. Polichetti, M.L. Addonizio, S. Aprea, C. Minarini and A. Rubini; Thin Solid Films, **354**, 73 (1999).

[8] E. Cazzanelli, S. Capoleoni and L. Papalino; Philosophical Magazine B, **82**, 453 (2002).

[9] E.Cazzanelli, L.Papalino, S. Capoleoni, R. Ceccato and G. Carturan, Ionics, **8**, 244 (2002).

[10] G. T. Went, S. T. Oyama and A. T. Bell; J. Phys. Chem., **94**, 4240 (1990).

[11] M.A. Vuurman and I.E. Wachs; J. Mol. Catal., **77**, 29 (1992).

[12] S. Lee, H. M. Cheong, M. J. Seong, P. Liu, C. E. Tracy, A. Mascarenhas, J. R. Pitts and S. K Deb; J. Appl. Phys., **92**, 1983 (2002).
[13] G. J. Exarhos and N.J. Hess; Thin Solid Films, **220**, 254 (1992).
[14] P.P. Lottici, D.Bersani, M. Braghini and A. Montenero; J. Mater. Science, **28,** 177 (1993).
[15] F.D. Hardcastle and I.E. Wachs; J. Phys. Chem., **95**, 5031 (1991).
[16] Y. Repelin, E. Husson, L. Abello and G. Lucazeau; Spectrochim. Acta, **41A,** 993 **(**1985).
[17] C. Julien, J. P. Guesdon, A. Gorenstein, A. Khelfa, and I. Ivanov; Applied Surface Science, **90**, 389 (1995).
[18] X. Zhang and R. Frech; Electrochim. Acta, **42**, 475 (1997).
[19] X. Zhang and R. Frech; J. Electrochem. Soc., **145**, 847 (1998).
[20] T. Ohsaka, F. Izumi and Y. Fujiki; J. Raman Spectr., **7**, 321 (1978).
[21] V. Bruno, E. Cazzanelli, N. Scaramuzza, G. Strangi, R. Ceccato and G. Carturan; J. of Applied Physics, **92 (9),** 5340 (2002).